Wood Sci Technol (2012) 46:579–590
DOI 10.1007/s00226-011-0423-1

ORIGINAL

Experimental and numerical investigations on adhesively bonded timber joints

Thomas Tannert · Till Vallée · Simon Hehl

Received: 18 January 2010 / Published online: 17 May 2011

Abstract Adhesively bonding of timber structural elements provides new opportunities as it is well adapted for the anisotropic and fibrous nature of the material. Experimental and numerical investigations were carried out on adhesively bonded full-scale double-lap joints composed of timber adherends (spruce) and adhesive layers. The influence of different geometric parameters and adhesives on the joint strength was studied. The investigated geometric parameters were the thickness of the adhesive layer (0.5–2.0 mm), the overlap length (40–280 mm), and the ductility of the adhesive (using three different adhesives). It was found that the joint strength was independent of the adhesive layer thickness (for the thickness range investigated) that the joint strength increased with the overlap length up to an apparent maximum of approximately 200 mm and that strength was almost independent of the adhesive stiffness. The numerical investigation was in good agreement with the experimental results and allows for the model to be used for strength prediction of the investigated joints.

Introduction

Adhesively bonded joints outperform connections achieved using dowel type mechanical fasteners in most of the cases; not only do they usually exhibit higher

T. Tannert (✉)
Department of Wood Science, University of British Columbia, 2424 Main Mall,
Vancouver, BC V6T1Z4, Canada
e-mail: thomas.tannert@gmx.net

T. Vallée
College of Architecture and Engineering, University of Applied Sciences Fribourg,
Fribourg, Switzerland

S. Hehl
Timber and Composite Construction, Bern University of Applied Sciences, Biel, Switzerland

capacities but also higher stiffnesses than mechanical connectors, the latter being of particular importance when the governing factor is serviceability limit state (SLS), as is it often with timber structures. Additional advantages of adhesively bonded joints were first recognized by the airplane and automotive industries. One of the most prominent early examples of adhesive joints was the de Havilland Mosquito aircraft which essentially consisted of plywood with substantial parts glued together (Moss 1946).

Although increasingly being used for fibrous and anisotropic materials, such as fiber reinforced polymers (FRP; e.g., Vallée et al. 2006), adhesive bonding is not yet widely applied for timber structural elements, despite its advantages. Before adhesive bonding can gain acceptance for the use in timber structures, methods need to be developed which predict the joint strength as a function of the material properties, the joint geometry, and the type of loading.

A prerequisite for the successful prediction of strength is the understanding of the stress–strain state in the joint; either analytically (by solving the differential equations describing the mechanics of the joint) or numerically (most commonly with the use of FEA). Contrary to analytical solutions, which are mostly restricted to idealized joints (da Silva et al. 2009a, b), FEA permits the consideration of all relevant geometrical details as well as the actual material behavior (Adams 1987; Tsai and Morton 1994; Keller and Vallée 2005).

The influence of different geometrical parameters (the overlap length and the adhesive layer thickness) on the strength of double-lap joints composed of FRP profiles was experimentally and numerically investigated (Keller and Vallée 2005; Vallée et al. 2006). The authors concluded that, within the considered thickness range, the adhesive layer thickness had only a small influence on the stress distribution and almost no influence on the joint strength. However, if considering analytical methods, e.g., Volkersen (1938) or Goland and Reissner (1944), higher adhesive layer thicknesses always lead to a joint strength increase (Adams and Comyn 2000). Gleich et al. (2001) however postulated the existence of an optimum adhesive layer thickness, for which joint strength is maximum, and which depends on the geometry and the materials involved (Vallée et al. 2009) have experimentally and numerically shown that such an optimum adhesive layer thickness exists for bonded FRP joints. Such evidence has not yet been reported for adhesively bonded joints of timber adherends.

Basic considerations lead to the fact that the easiest way to reduce stress peaks, and thus increase joint capacity, is using a mechanically plastic adhesive, as shown by different authors, the first one to publish such results was Hart-Smith who used a bi-linear elastic perfectly plastic model approximation (Hart-Smith 1973, 1974). Bigwood and Crocombe (1990) experimentally showed that adhesives with plastic material properties lead to reductions of shear stresses along the overlap of investigated bonded joints, which were in good agreement with results obtained by FEA. For adhesively bonded timber joints, no conclusive studies regarding the effect of the adhesive stiffness and ductility on joint capacity are available.

This paper describes the results of experimental and numerical investigations concerning the influence of geometrical parameters, namely the overlap length, the adhesive layer thickness, and compares brittle elastic adhesives with ductile ones;

the influence of the latter on the capacity of adhesively bonded joints involving timber adherends is pointed out.

Experimental investigation

Specimen description

Symmetrical double-lap joints consisting of two outer and two inner timber boards (adherends) with rectangular sections connected by a layer of adhesive were fabricated. To keep the cumulative cross-section constant, the inner adherends were always twice as thick as the outer ones with $t_i = 38$ mm and $t_0 = 19$ mm, respectively. The width of the adherends was kept constant at 50 mm. Adhesive thickness was ensured through the use of calibrated PVC shims.

In the frame of the investigations presented herein, three parameters were varied:

- The overlap length L (40–280 mm in steps of 40 mm);
- The thickness of the adhesive layer t_a (0.5, 1.0, and 1.5); and
- The adhesive; three different types (A–C, detailed subsequently) with different stiffness and ductility.

Figure 1 details the used nomenclature while Table 1 shows the parameter combinations of the investigated joints.

Material

The timber species used was spruce (*Picea abies*) cut from high quality almost defect-free boards. The material was conditioned to 12% moisture content prior to manufacturing of the specimens, and then again stored in constant climate until testing. The material was considered orthotropic with identical properties in radial and tangential directions. The elastic properties required for the subsequent numerical investigations (longitudinal modulus of elasticity E_X and transverse modulus of elasticity E_Y) were determined on specimens cut from the same boards that were used to produce the joints. Table 2 summarizes the results.

Three different adhesives were considered in the frame of the investigations reported herein: a stiff and brittle 2C epoxy—SikaDur330 (Type A); a 2C polyurethane adhesive exhibiting some plasticity—SikaForce7851 (Type B); and an

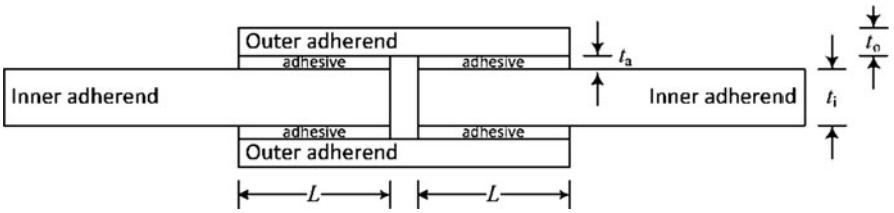

Fig. 1 Geometry of double-lap joint specimens (not to scale)

Table 1 Overview of joint configuration and experimental results

Adhesive	L [mm]	t_a [mm]	No of specim.	F_{ult} [kN]	F_{ult} COV (%)
Type A	40	1.0	6	13.6	14
Type A	80	1.0	6	20.9	18
Type A	120	1.0	6	25.4	25
Type A	160	0.5	3	36.7	7
Type A	160	1.0	6	32.7	23
Type A	160	1.5	3	35.3	13
Type A	200	1.0	6	33.7	18
Type A	240	1.0	6	33.0	11
Type A	280	1.0	6	36.1	14
Type B	80	1.0	3	25.9	10
Type B	120	1.0	3	36.2	8
Type B	160	0.5	3	36.2	20
Type B	160	1.0	3	38.3	14
Type B	160	1.5	3	41.5	7
Type C	80	1.0	3	25.6	12
Type C	120	1.0	3	32.7	11
Type C	160	0.5	3	37.5	24
Type C	160	1.0	3	38.4	24
Type C	160	1.5	3	38.9	7

Table 2 Overview of material properties

Material	E_X [MPa]	E_Y [MPa]	E_P^a [MPa]	υ_{XY}^b [−]	$\upsilon_{YZ} = \upsilon_{YZ}^b$ [−]
Timber	17,910	1,120		0.40	0.04
Type A	4,563			0.37	
Type B	586		31	0.42	
Type C	141		14	0.40	

[a] Modulus beyond elastic limit

[b] According to Green et al. (1999)

acrylic adhesive exhibiting major plasticity—SikaFast5221 (Type C). The fundamentally different mechanical properties are best represented in Fig. 2, which depicts the idealized stress–strain relationship in tension, as derived from EN ISO 527-2 tests. Table 2 lists the relevant mechanical parameters.

Methods

All experiments on the adhesively bonded joints were performed in a universal testing machine as quasi-static axial tensile tests under a displacement-controlled rate of 5 mm/s, up to failure, within controlled laboratory conditions (approx. 20°C

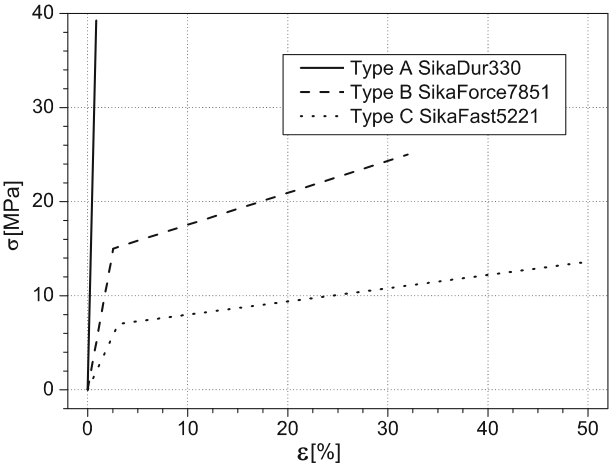

Fig. 2 Idealized mechanical description in tension of the adhesives used

and 50% relative humidity). The specimens were cut in dog-bone shapes (reducing the width and depth in the center parts) to avoid premature failure in the clamped zones. For all specimens, the load displacement behavior was measured and recorded up to the maximum load (F_{ult}).

Analysis of variance (ANOVA) was carried out to evaluate the effect of the parameters on F_{ult}. ANOVA provides a statistical test of whether or not the means of the several test series exhibit significant differences. Based on the number of observations, a p value is calculated and compared with the significance level, α, typically chosen as 0.05. If the p value is smaller than α, then the hypothesis of no differences between means is rejected and the observed difference in means is significant (Montgomery and Runger 2003).

Experimental results

Figure 3 shows the joint load vs. relative deformation response of the joints involving the softest adhesive (Type C) with an overlap length $L = 80$ mm. It can be clearly observed that, even for the most ductile adhesive tested, the structural response is linear up to failure, with almost no system ductility.

All investigated adhesively bonded joints failed in a brittle manner, independent from the ductility of the adhesive used. Failure always occurred in the adherends—in no single case did the adhesive layer fail. Joints almost always failed by splitting just below the end of the overlap, as illustrated in Fig. 4; this corresponds to a stress singularity in the joints, as subsequently shown by the FEA. The average values and standard deviations of the failure loads, F_{ult}, measured are listed in Table 1. The test results can be summarized as follows:

1. Joint strength is positively correlated with the overlap length, L, as shown in Table 1 and Fig. 5; however, the strength increase is not linear but

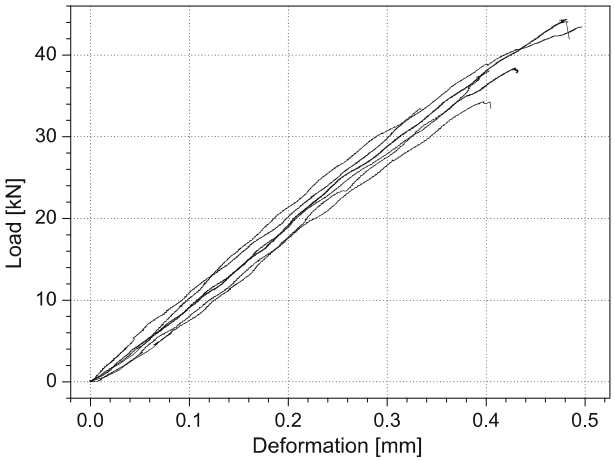

Fig. 3 Load-deformation response of adhesively bonded timber joints

Fig. 4 Typical specimen after testing: close-up at the locus of failure initiation

asymptotically approaches a maximum value. Beyond 160 mm overlap length, no significant joint strength increases are noticed.

2. Joint strength is almost independent of the adhesive layer thickness, at least within the range of investigated data, as indicated in Table 1 and Fig. 6.
3. Joint strength seems slightly dependent on the adhesive ductility; the very stiff epoxy results in slightly lower joint strengths, shown in Table 1 and Fig. 7.
4. The overall scattering of the strengths amounts for around 15% and is comparable for all investigated series, ranging from 7 to 25%.

ANOVA at a level $\alpha = 0.05$ was applied to statistically evaluate the results. Table 3 gives a summary of the obtained p values. The overlap length has a

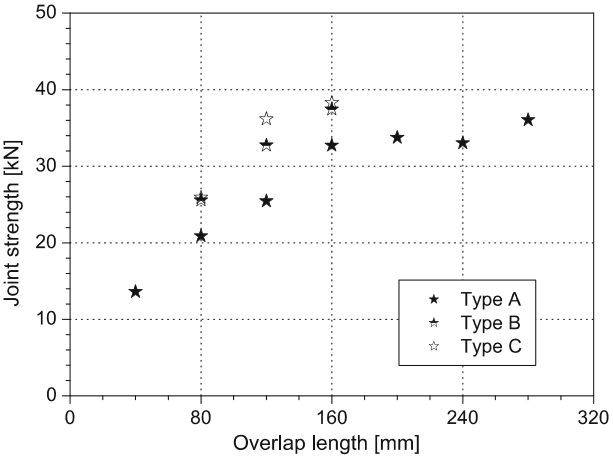

Fig. 5 Experimentally determined joint strengths versus overlap length for different adhesives

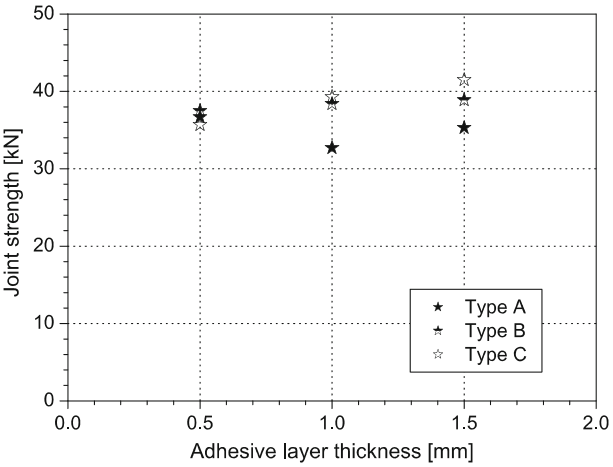

Fig. 6 Experimentally determined joint strengths versus adhesive thickness for different adhesives

significant effect on joint strength for all three investigated adhesives. Multiple comparison tests (Least Square Differences at a level $\alpha = 0.05$) showed no significant differences in strength beyond 160 mm overlap for adhesive Type A and beyond 120 mm overlap for adhesive Types B and C. Within the range of investigated values, the adhesive layer thickness has no statistically significant effect on joint strength for all overlap lengths and adhesive types. The adhesive stiffness has a significant effect for the overlap length 120 mm. Here, the stiff adhesive (Type A) results in lower joints strengths. For the smaller and the longer overlaps (80–160 mm), the adhesive stiffness has no significant effect on joints strength.

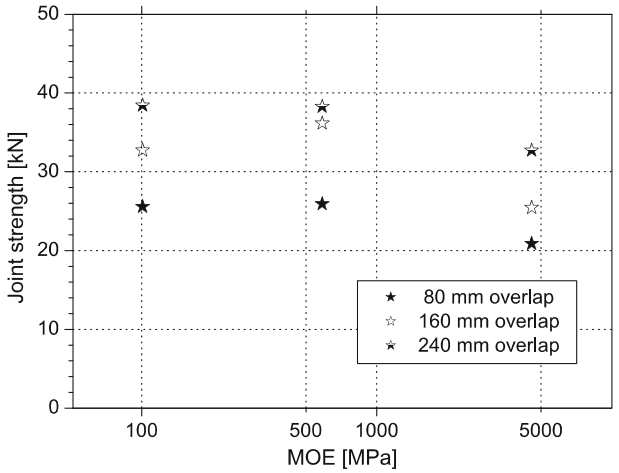

Fig. 7 Experimentally determined strengths versus adhesive stiffness for different overlap lengths

Table 3 ANOVA summary

Parameter combination	*p* value
Overlap length (type A)	**<0.001**
Overlap length (type B)	**0.015**
Overlap length (type C)	**0.050**
Adhesive thickness (type A)	0.643
Adhesive thickness (type B)	0.524
Adhesive thickness (type C)	0.975
Adhesive type (80 mm overlap)	0.094
Adhesive type (120 mm overlap)	0.048
Adhesive type (160 mm overlap)	0.431

Numerical investigation

Numerical model for adhesively bonded double-lap joints

All joint configurations were modeled using the Finite Element program ANSYS (v11). Timber is an anisotropic and inhomogeneous material, but for simplicity in modeling, the material was assumed to be homogeneous and transverse isotropic with identical properties in radial and tangential directions. The longitudinal direction is referred to as parallel to grain (herein defined by the subscript X) while the combined radial and tangential directions are referred to as perpendicular to grain (subscript Y).

Previous studies on adhesively bonded joints (e.g., Richardson et al. 1993; Andruet et al. 2001; Vallée et al. 2006; Hua et al. 2008) showed that 2D instead of 3D modeling is accurate enough, since all relevant stress components are almost equally distributed over the width. Consequently, 2D 8-node orthotropic elements

were used. Symmetry conditions were used to reduce the modeling to one quarter. Just below the end of the overlaps, where failure initiation was observed, a very fine quadratic mesh (element size 0.25 mm) was applied to allow for an accurate modeling of the stresses in this critical region.

Since brittle failure occurred within the elastic range of the timber, the latter was considered linear elastic, with the mechanical properties listed in Table 2. The adhesives were modeled according to Fig. 2 using the properties also listed in Table 2, leading to non-linear calculations for both adhesive types B and C. All calculations were performed at the mean experimentally gathered strength value.

Results of numerical modeling

Since failure clearly initiated in the inner adherend, it was decided to gather the profiles of both the perpendicular to the grain stresses, σ_Y, and in-plane shear stresses, τ_{XY}, along the bonded splice of the inner adherend for the geometrical configurations investigated herein. Figure 8 shows the computed stresses along the previously defined path at joint capacity.

Considering increasing overlap lengths, both σ_Y and τ_{XY}, peak independently of the overlap length at comparable magnitudes (on average 28 MPa for σ_Y, and around 18 MPa for τ_{XY}). Further, the σ_Y-stress profiles are very similar in regard to the overlap length. With increasing overlap lengths, the shear stress profiles become steeper; at $L = 80$ mm, for example, shear stresses range around 2.2 MPa over a large portion of the overlap, at $L = 240$ mm their value has dropped to below 0.7 MPa, with almost no shear stress plateau.

Both perpendicular to the grain stresses, σ_Y, and in-plane shear stresses, τ_{XY}, are almost identical at each of the three considered adhesive layer thicknesses, t_a, if considered at their respective experimentally determined capacity. The σ_Y-stress peaks at the end of the overlap, where failure was observed, amount for 28 MPa on average, with differences below 1% considering t_a from 0.5 to 1.5 mm; similarly, for shear, τ_{XY}, the peaks at the same location amounted for 18 MPa, also with differences below 1% for the thicknesses investigated.

Figure 8 clearly indicates that with decreasing stiffness of the adhesive, considering adhesive Type A to Type C, the peak values of the perpendicular to the grain stresses, σ_Y, at the end of the overlap are significantly reduced: 28 MPa for Type A, 12 MPa for Type B, and 6 MPa for Type C. Similar stress reductions can be noticed for the shear stresses, τ_{XY}, at the end of the overlap (from 18 to 3 MPa, if switching from Type A to Type C). Moreover, the shear stress profiles tend to flatten with decreasing adhesive stiffness, leading for the softest adhesive, Type C, to a largely flat shear stress profile along the overlap, which greatly contrasts with the sharp stress peaks observed for adhesive Type A.

Discussion

Experimental investigations showed that load deformation response of adhesively bonded timber joints under axial tension loading is linear until failure, including the

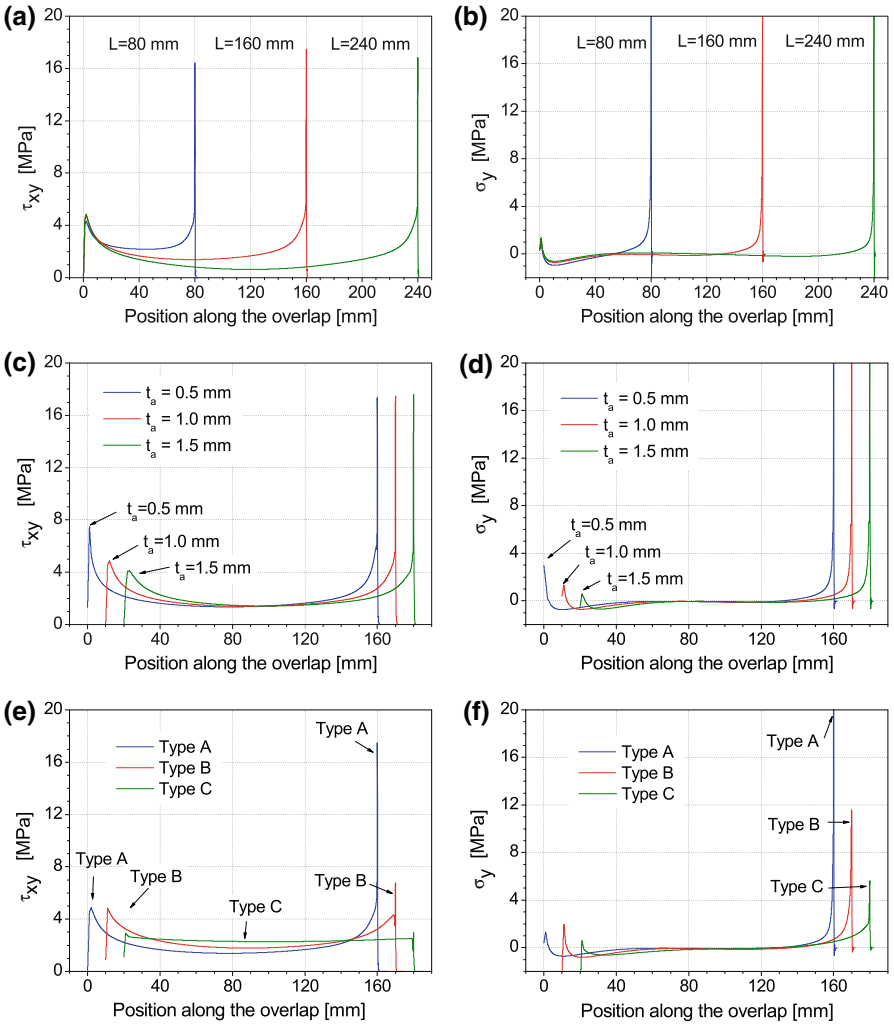

Fig. 8 Stresses along the overlap in the inner adherend: for different overlap lengths (**a** and **b**), for different adhesive layer thicknesses (**c** and **d**) and for different adhesive stiffnesses (**e** and **f**) Note: parts **c**, **d**, **e**, and **f** are plotted with a 10-mm offset between individual curves

cases where ductile adhesives were used; joints always failed in a brittle manner in the timber adherends. The experimental study further indicated that joint strength increased proportionally to the overlap length up to a critical overlap length (here, around 160 mm for the stiff adhesive and 120 mm for the adhesives exhibiting plasticity) beyond which no significant further increase was achieved. A statistical analysis confirmed these findings. It was shown that for all investigated overlap lengths, L, and for all adhesive layer thicknesses, t_a, the magnitudes of the perpendicular to the grain stresses, σ_Y, and in-plane shear stresses, τ_{XY}, at joint capacity were very comparable.

The adhesive stiffness influenced the joint strength slightly and only at one level of overlap lengths ($L = 120$ mm); beyond and below that overlap length, no significant differences were observed, even using the adhesive Type C exhibiting major plasticity. On the other hand, if considering differences in the adhesive ductility and also at joint capacity, both σ_Y- and τ_{XY}-stresses undergo significant changes; the magnitudes of the maxima are reduced by around 60% for adhesive Type B and 80% for Type C, if compared with the stiffest adhesive used (Type A). The experimental evidence therefore shows that neither the stiffness nor the plasticity of the adhesive had a significant influence on the strength of the corresponding bonded joints; despite the fact that FEA clearly indicates that stresses were significantly reduced.

Beyond the latter considerations, the numerical calculations showed that at their respective failure loads, the magnitude of the highest out-of-plane tension stress (perpendicular to the grain), σ_Y, and in-plane shear stresses, τ_{XY}, is far beyond the generally accepted thresholds of material strength under uniform stress.

As a consequence, a criterion based on maximum stress cannot be used to predict the joint strength. Besides the stress maxima, it is postulated that the stress distributions (stress gradients and volume subjected to high stresses) must also influence the strength. It is therefore hypothesized that size effect must influence joint strength, an assumption that was investigated by Tannert et al. (2011).

Conclusion

Experimental and numerical investigations were carried out to study the influence of parameters on the strength of adhesively bonded timber joints. The following conclusions were drawn: (1) the experimental work, in conjunction with the corresponding numerical analysis, strongly indicates that the joint failures were initiated by a combination of local tension perpendicular to the grain and shear stresses at the joint edges in the adhesive interface; (2) comparisons between numerical and experimental results show that the model is reliable in predicting the structural response, suggesting that it can be used to develop a numerical based method to predict failure loads.

However, it appears that the joint strength is not directly correlated to the stress-state, so that simple stress-based dimensioning methods fail. The experimental and numerical work presented herein gathered data to benchmark a dimensioning method, which, in conjunction with additional material-specific tests to determine an appropriate failure criterion, offers a dimensioning method.

References

Adams RD (1987) Theoretical stress analysis of adhesively bonded joints. In: Matthews FL (ed) Joining fiber-reinforced plastics. Elsevier Applied Science, Essex

Adams RD, Comyn J (2000) Joining using adhesives. Assembl Autom 20(2):109–117

Andruet RH, Dillard DA, Holzer SM (2001) Two- and three-dimensional geometrical nonlinear finite elements for analysis of adhesive joints. Int J Adhesion Adhesives 21(1):17–34
Bigwood DA, Crocombe AD (1990) Nonlinear adhesively bonded joints design analysis. Int J Adhesion Adhesives 10(1):31–41
Da Silva LFM, Das Neves PJC, Adams RD, Wang A, Spelt JK (2009a) Analytical models of adhesively bonded joints—part II: comparative study. Int J Adhesion Adhesives 29(3):331–341
Da Silva LFM, Das Neves PJC, Adams RD, Spelt JK (2009b) Analytical models of adhesively bonded joints—part I: literature survey. Int J Adhesion Adhesives 29(3):319–330
Gleich DM, Van Tooren MJL, Beukers A (2001) Analysis and evaluation of bond line thickness effects on failure load in adhesively bonded structures. J Adhes Sci Technol 15(9):1091–1101
Goland M, Reissner E (1944) The stresses in cemented joints. J Appl Mech 11:A17–27
Green DW, Winandy JE, Kretschmann DE (1999) Mechanical properties of wood. In: Wood handbook—wood as an engineering material. General technical report FPL; GTR-113. Forest Products Laboratory, Madison, WI, USA, p 463
Hart-Smith LJ (1973) Adhesively bonded single-lap joints. NASA CR-112236
Hart-Smith LJ (1974) Analysis and design of advanced composite bonded joints. NASA CR-2218
Hua Y, Crocombe AD, Wahab MA, Ashcroft IA (2008) Continuum damage modelling of environmental degradation in joints bonded with EA9321 epoxy adhesive. Int J Adhesion Adhesives 28(6):302–313
Keller T, Vallée T (2005) Adhesively bonded lap joints from pultruded GFRP profiles part I: stress–strain analysis and failure modes. Compos B 36:331–340
Montgomery DC, Runger GC (2003) Applied statistics and probability for engineers. Wiley, New York
Moss CJ (1946) Aeronautical engineering—bonding with Redux, The Aeroplane, no. 329
Richardson G, Crocombe AD, Smith PA (1993) A comparison of two-and three-dimensional finite element analyses of adhesive joints. Int J Adhesion Adhesives 13(3):193–200
Tannert T, Vallée T, Hehl S (2011) Probabilistic strength prediction of adhesively bonded timber joints. Wood Sci Technol. doi:10.1007/s00226-011-0424-0
Tsai MY, Morton J (1994) An evaluation of analytical and numerical solutions to the single-lap joint. Int J Solids Struct 31(18):2537–2563
Vallée T, Correia JR, Keller T (2006) Probabilistic strength prediction for double lap joints composed of GFRP profiles, part I: experimental and numerical investigations. Compos Sci Technol 66:1903–1914
Vallée T, Correia JR, Keller T (2009) Optimum thickness of joints made of GFPR pultruded adherends and polyurethane adhesive. Compos Struct. doi:10.1016/j.compstruct.2009.09.056
Volkersen O (1938) Die Nietkraftverteilung in zugbeanspruchten konstanten Laschenquerschnitten. Luftfahrtforschung 15:41–47